

In vitro Dosimetric Study of Biliary Stent Loaded with Radioactive ^{125}I Seeds

Li-Hong Yao¹, Jun-Jie Wang¹, Charles Shang^{2,3}, Ping Jiang¹, Lei Lin¹, Hai-Tao Sun¹, Lu Liu¹, Hao Liu⁴, Di He⁵, Rui-Jie Yang¹

¹Department of Radiation Oncology, Peking University Third Hospital, Beijing 100191, China

²Department of Physics, Florida Atlantic University, Boca Raton, FL 33431, USA

³Department of Radiation Oncology, Lynn Cancer Institute, Boca Raton, FL 33486, USA

⁴Department of Computer Science and Engineering, University of Washington, Seattle, WA 98195, USA

⁵LMAM, School of Mathematical Sciences, Peking University, Beijing 100871, China

Abstract

Background: A novel radioactive ^{125}I seed-loaded biliary stent has been used for patients with malignant biliary obstruction. However, the dosimetric characteristics of the stents remain unclear. Therefore, we aimed to describe the dosimetry of the stents of different lengths — with different number as well as activities of ^{125}I seeds.

Methods: The radiation dosimetry of three representative radioactive stent models was evaluated using a treatment planning system (TPS), thermoluminescent dosimeter (TLD) measurements, and Monte Carlo (MC) simulations. In the process of TPS calculation and TLD measurement, two different water-equivalent phantoms were designed to obtain cumulative radial dose distribution. Calibration procedures using TLD in the designed phantom were also conducted. MC simulations were performed using the Monte Carlo N-Particle eXtended version 2.5 general purpose code to calculate the radioactive stent's three-dimensional dose rate distribution in liquid water. Analysis of covariance was used to examine the factors influencing radial dose distribution of the radioactive stent.

Results: The maximum reduction in cumulative radial dose was 26% when the seed activity changed from 0.5 mCi to 0.4 mCi for the same length of radioactive stents. The TLD's dose response in the range of 0–10 mGy irradiation by ^{137}Cs γ -ray was linear: $y = 182225x - 6651.9$ ($R^2 = 0.99152$; y is the irradiation dose in mGy, x is the TLDs' reading in nC). When TLDs were irradiated by different energy radiation sources to a dose of 1 mGy, reading of TLDs was different. Doses at a distance of 0.1 cm from the three stents' surface simulated by MC were 79, 93, and 97 Gy.

Conclusions: TPS calculation, TLD measurement, and MC simulation were performed and were found to be in good agreement. Although the whole experiment was conducted in water-equivalent phantom, data in our evaluation may provide a theoretical basis for dosimetry for the clinical application.

Key words: Brachytherapy; Computer Simulation; Phantom; Radiometry; Thermoluminescent Dosimetry

INTRODUCTION

Clinical management of malignant biliary obstruction remains challenging. For these patients, minimally invasive biliary stenting is often preferred. However, restenosis due to tumor ingrowth or compression is a problem.^[1] External beam radiotherapy (EBRT) has been used to prolong stent patency, but almost inevitably results in normal tissue toxicity because of the proximity of vital organs. More recently, good results have been reported with the use of a combination of intraluminal ^{192}Ir brachytherapy and stenting.^[2-5]

Address for correspondence: Dr. Jun-Jie Wang,

Department of Radiation Oncology, Peking University Third Hospital,

Beijing 100191, China

E-Mail: junjiawang_edu@sina.cn

The content of this paper has been presented in the 2016 World Congress of Brachytherapy as an ePoster and then been published in Brachytherapy (15/Supplement/S162) as an abstract style.

This is an open access article distributed under the terms of the Creative Commons Attribution-NonCommercial-ShareAlike 3.0 License, which allows others to remix, tweak, and build upon the work non-commercially, as long as the author is credited and the new creations are licensed under the identical terms.

For reprints contact: reprints@medknow.com

© 2017 Chinese Medical Journal | Produced by Wolters Kluwer - Medknow

Received: 28-12-2016 **Edited by:** Yuan-Yuan Ji

How to cite this article: Yao LH, Wang JJ, Shang C, Jiang P, Lin L, Sun HT, Liu L, Liu H, He D, Yang RJ. *In vitro* Dosimetric Study of Biliary Stent Loaded with Radioactive ^{125}I Seeds. Chin Med J 2017;130:1093-9.

Access this article online

Quick Response Code:



Website:
www.cmj.org

DOI:
10.4103/0366-6999.204936

Recently, low-dose rate ^{125}I seed-loaded intraluminal stents have been developed. Zhu *et al.*^[6] were the first to report encouraging results with its clinical application. However, seed activity, reference point of prescription dose, and the irradiation dose of target were different in the related studies.^[6,7] Therefore, comparison of clinical efficacy among different studies becomes difficult. The American Association of Physicists in Medicine (AAPM) Task Group No. 60 and 149 reports recommend that, for each type of radioactive stent (i.e., of various lengths, diameters, and activities), the three-dimensional (3D) dose distributions should be carefully determined before clinical application.^[8,9] However, there are limited reports that describe the dosimetry of the stents.

In this study, we aimed to use the treatment planning system (TPS) calculation, thermoluminescent dosimeter (TLD) measurement, and Monte Carlo (MC) simulation to evaluate the characteristics of dosimetric distribution of the novel radioactive stents of different lengths — with different number as well as activities of ^{125}I seeds — and to provide a theoretical basis for dosimetry for the clinical application.

METHODS

Radioactive ^{125}I source

The geometry of model 6711 ^{125}I seed used in this study was provided by the manufacturer (HTA Co., Ltd, Beijing, China). The source capsule consisted of a 0.05-mm-thick titanium cylinder ($\rho = 4.54 \text{ g/cm}^3$), 4.5 mm long \times 0.8 mm in diameter, and with end-weld thickness of 0.4 mm, containing a silver core ($\rho = 10.5 \text{ g/cm}^3$) of 3.0 mm length and 0.5 mm diameter, onto which a 1- μm layer of ^{125}I had been uniformly absorbed. Source activity was in the range of 0.1–6.0 mCi. The dosimetric characteristics of a single model 6711 ^{125}I source in a homogeneous water medium has been previously investigated by several groups.^[10,11]

Radioactive stent model

The radioactive stent was designed as two separate parts: an inner 8-mm diameter conventional self-expanding biliary nitinol stent to provide support and an outer 10-mm diameter radioactive self-expandable stent loaded with ^{125}I seeds [Nanjing Microinvasive Medical Inc., Nanjing, China; Figure 1a]. Each seed casing, 10 mm long and 0.8 mm in diameter, tightly holds the radioactive seed. The minimal distance between two adjacent radioactive seeds is approximately 7.1 mm in the cross-sectional view [center to center; Figure 1b] and 10.0 mm in the longitudinal direction [end to end; Figure 1c]. In this investigation, three representative models of 4 cm, 6 cm, and 8 cm length loaded with 8, 16, and 24 ^{125}I seeds, respectively, were studied. In addition, various radioactive strengths, ranging from 0.4 to 1.0 mCi per seed (in 0.1-mCi increments), were evaluated independently.

Treatment planning system calculation

This process and the equivalent model have been described in detail in a previous published paper.^[12] In brief, solid

paraffin ($\rho = 0.880\text{--}0.915 \text{ g/cm}^3$, Leica, Germany), welded to a polymethylmethacrylate (PMMA) cylindrical barrel of 15-cm height and 20-cm diameter, was used as the water-equivalent phantom. The stent loaded with dummy ^{125}I sources (model 6711; China Isotope Corporation, Beijing, China) was vertically mounted at the bottom of the barrel. For CT scan, the cylindrical PMMA barrel was mounted on a head immobilization. Scans were performed with 5-mm slice thickness and spacing to cover the entire length of the stent. DICOM images were sent to the TPS (Prowess - 3D, SSGI, USA) for contouring and planning. Calculation points were selected from polar angles ranging from 0° to 360° in 45° increments and at radial distances ranging from 1 cm to 8 cm in 0.5-cm increments and points of 1.25 and 1.75 cm. Thus, each data point represented the average of the eight calculations.

Thermoluminescent dosimeter measurement

Radial dose distribution around the stents was measured in a PMMA phantom using TLD-GR 200A (Beijing Guangtong Yirun radiation monitoring equipment Co., Ltd.) circular chips of 0.8-mm thickness and 4.5-mm diameter. Before exposure, all the TLDs were annealed at 240°C for 10 min, and then fast cooled. Annealing was repeated as necessary to complete all measurements. The irradiated TLDs were read 24–48 h postirradiation using an automated TLD reader (CTLD-350; Institute of Radiation and Radiation Medicine, Military Medical Science Academy of the PLA). An initial TLD calibration reading was made to study the TLD's linearity of dose response and energy response scaled for exposure duration. To study the dose response of the TLDs, irradiation was performed with a standard ^{137}Cs (662 keV γ -ray) irradiator at the Standard Dosimetry Laboratory (China Institute of Atomic Energy Metering Station, Beijing). In the process, 10 TLDs were used for each configuration of 0.5 mGy, 1 mGy, 2 mGy, 5 mGy, and 10 mGy. As the energy of emitted photons of ^{125}I is in the range of 7.2–35.5 keV,^[10,11] 33 keV, 65keV, and 83 keV narrow-spectrum X-ray standard radiation sources, ^{241}Am (59.5 keV γ -ray) and 6 MV X-ray (Axesse™ Linear Accelerator, Elekta Medical Systems, Sweden) were selected to irradiate each group of 10 TLDs to a dose of 1 mGy to measure the TLD's energy response.

A water-equivalent PMMA phantom was constructed to provide full scattering conditions with thirty pieces of 30 cm \times 30 cm \times 1 cm slabs. For the central phantom slab to accommodate the circular TLD chips, there was a hole (1.2 cm in diameter) in the center where the radioactive stents could be placed. The square holes (5.0 mm long, 2.0 mm wide, and 4.5 mm deep) were drilled such that the TLD surface would be perpendicular to the slab plane and with the centers of the dosimeters being parallel to the long axis of the source. The whole pattern of the spiral configuration was chosen to minimize inter-dosimeter attenuation and perturbation effects.^[13,14] The dosimeters were positioned at radial distances of 1 cm to 8 cm in 0.5-cm increments, points of 1.25 and 1.75 cm, and polar angles

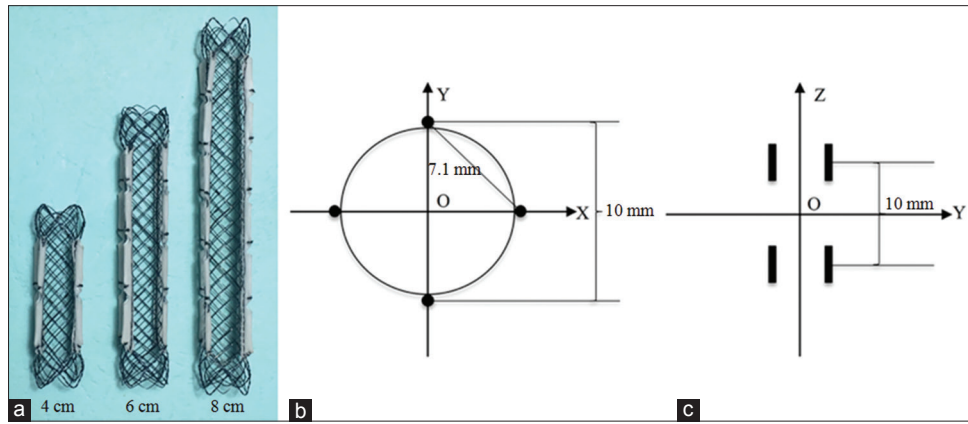


Figure 1: Location map of radioactive biliary stents in a rectangular coordinate system. (a) Photograph of the radioactive biliary stent. (b) A cross-sectional view of the biliary stent. (c) Seeds' location in a longitudinal view of a stent of 4-cm length.

ranging from 0° to 90° in 10° , with respect to the stent's long axis. Each dosimetric data point represented the average of the four TLD measurements. All measurements were performed within 24 h after in-phantom exposures^[15] and repeated thrice to increase the confidence level.

According to the AAPM TG43,^[10] the dose rate in water surrounding a ^{125}I source can be calculated as follows:

$$\dot{D}(r, \theta) = S_k \cdot \Lambda \cdot \frac{G(r, \theta)}{G(r_0, \theta_0)} \cdot g(r) \cdot F(r, \theta) \quad (1)$$

where, S_k is the air kerma strength given by $S_k = k \cdot A_0 \cdot e^{-\lambda t}$, k is the air kerma conversion factor, A_0 is the initial activity, and λ is the decay constant of ^{125}I . Therefore, the cumulative absorbed dose in interest points over a period of time can be calculated as follows:

$$D_t(r, \theta) = \int_0^t k \cdot A_0 \cdot e^{-\lambda t} \cdot \Lambda \cdot \frac{G(r, \theta)}{G(r_0, \theta_0)} \cdot g(r) \cdot F(r, \theta) dt = \dot{D}_0(r, \theta) \frac{(1 - e^{-\lambda t})}{\lambda} \quad (2)$$

where, $\dot{D}_0(r, \theta)$ is the initial dose rate of the interest point. The measured dose rate from the TLD responses from each point irradiated in the phantom was calculated as follows:

$$\dot{D}_0(r, \theta) = \frac{R \cdot C_f \cdot S_{\text{AD,med}}^{\text{rel}} \cdot P_{\text{phant}} \cdot \lambda}{(1 - e^{-\lambda t})} \quad (3)$$

where, R is the reading of the TLDs (nC), C_f is the calibration factor for the TLD response (mGy/nC), $S_{\text{AD,med}}^{\text{rel}}$ is the relative absorbed dose sensitivity of the TLD to establish the equivalent dose to water per unit reading in the ^{125}I field, P_{phant} is the phantom correction factor to derive the corresponding dose to water in water from the ^{125}I seed, and t is in-phantom exposure time equaling to 24 h. $S_{\text{AD,med}}^{\text{rel}}$ and P_{phant} were taken from literature^[16] to be 1.51 and 0.898, respectively. All the irradiations were in the linear response region of the TLDs, so no correction was necessary for the supralinearity effect.

Monte Carlo simulation

The Monte Carlo N-Particle eXtended (MCNPX) (version 2.5) code, which transports many particle types at almost all energies, was used to simulate the movement of photons with random positions, directions, and energy in the given region to calculate the stent's 3D dose rate distribution in liquid water. The MC simulations were performed for comparison with the TPS calculations and TLD measurements at 0.5–10.0 cm from stent surface.

In this investigation, the ^{125}I photon spectra were adopted from the AAPM TG43U1 report.^[11] The recommended photons per disintegration of ^{125}I are 0.406 (27.202 keV), 0.757 (27.472 keV), 30.98 (0.202 keV), 31.71 (0.0439 keV), and 0.0668 (35.492 keV).^[11] The radioactive stent model was centered in a 30 cm water-equivalent ($\rho = 0.998 \text{ g/cm}^3$) cylinder adequate for all the scattering effects from the surrounding medium. For scoring the 3D dose rate distribution of the radioactive stent, the cylinder was divided into a set of concentric rings with different widths and thicknesses. For scoring the radial dose rate distribution at different distances from the radioactive stent surface, the width and thickness of the ring were 0.1 mm for distances to the surface of the stent <1 cm, 0.2 mm for distances of 1–2 cm, 0.3 mm for distances of 2–3 cm, and 0.5 mm for distances of 3–10 cm. For scoring the axial dose rate distribution in the yz plane [Figure 1c] from $z = 0 \text{ cm}$ to $y = z = 10 \text{ cm}$, the width and thickness of the ring were 0.1 mm for distances to the center of the stent of <2 cm, 0.2 mm for distances of 2–3 cm, and 0.5 mm for distances of 3–10 cm. Due to the cylindrical symmetry, the dose rate distribution at z and $-z$ (at equal to y) is the same. ^{125}I seeds, water-equivalent cylinder, and tally cells were determined in the same coordinates [Figure 1c].

Every ^{125}I seed was simulated as a line source by the AAPM TG43 approximation, and using the MCNP F4 tally (particles/cm²), particle tracks and relative properties were recorded in each cylindrical annulus. Energy fluency was converted into dose rate using the dose energy (DE), dose function (DF), and tally multiplier (Fm) cards. The photon interaction cross-section file used in this study was

the DLC-200 library, distributed by the Radiation Shielding Information Computing Center (Oak Ridge, TN, USA). Evaluation of radial and axial dose rates was performed with 10^8 photon histories in water to comply with good MC practice recommendations^[11] regarding statistical uncertainty. The photon cutoff energy was set to 1 keV.

Statistical analysis

Statistical analysis was conducted using IBM SPSS for Windows, version 19.0 (IBM Corp., Armonk, NY, USA). Analysis of covariance was used to examine the factors influencing radial dose distribution of the radioactive stent. Two-tailed $P < 0.05$ was considered statistically significant.

RESULTS

Factors influencing cumulative radial dose

For TPS results, the relative errors of the three time measurements were $<3\%$. When the activity of the ^{125}I seeds remained the same, the length of the stent or the number of radioactive seeds affected cumulative radial dose significantly ($F = 14.704, P < 0.001$). When the stent length changed from 8 cm to 6 cm, the cumulative radial dose decreased by 6–44%, and when the length changed from 6 cm to 4 cm, the decrease was 34–97%. For the same length of radioactive stent, the cumulative radial dose changed significantly ($F = 35.510, P < 0.001$) when the seed activity was altered by 0.1 mCi or more. When the source strength changed from 0.5 mCi to 0.4 mCi, the percentage of the cumulative radial dose reduction was the largest for the same length of radioactive stents, and the maximum dose reduction for the three radioactive stents in this study was 26%.

Comparison of the three methods

Since the dose rate is linearly related to activity of the radioactive seeds, in the TLD measurement and MC simulation, only 0.4 mCi ^{125}I seeds were employed in this study. Our data show that the TLD's dose response in the range of 0–10 mGy irradiation by ^{137}Cs γ -ray was linear: $y = 182225x - 6651.9$ ($R^2 = 0.99152$; y is the irradiation dose in mGy, x is the TLDs' reading in nC). For the TLDs energy response, when TLDs were irradiated by different energy radiation sources to a dose of 1 mGy, reading of TLDs was different [Table 1]. For TLD results with the measured data, the calibration factor C_f for the TLD response in our work was 0.0012 mGy/nC; the relative error of the TLD measurements of radial dose rate was $<6\%$.

In this experiment, when the 4-cm stents loaded with 8 ^{125}I seeds were simulated (single seed activity, 0.4 mCi), the MCNPX-derived values of radial dose rate agreed to be within 5.7% of the TPS results and to be within 7.0% of the TLD measurements for most of the data points. For the 6-cm and 8-cm stents loaded with 16 and 24 ^{125}I seeds, respectively, the corresponding values were 6.9% and 7.0% and 7.3% and 6.7%, respectively. As shown in Figure 2, the simulations by MCNPX agreed well with the TPS calculations and TLD measurements.

Table 1: Energy response of TLD to irradiation by standard energies of different radiation sources

Radiation sources	Relative value
33 keV (X-ray)	1.23
^{241}Am (59.5 keV)	1.22
65 keV (X-ray)	1.14
83 keV (X-ray)	1.02
^{137}Cs (662 keV)	1.00
6 MV (X-ray)	1.28

Energy response values were normalized to TLD's reading for ^{137}Cs irradiation. TLD: Thermoluminescent dosimeter.

3D dose rate simulated by Monte Carlo N-Particle eXtended

For the three stent models, the 3D dose rates along the axial axis as estimated by MCNPX simulations are shown in Figure 3. Using these dosimetry data, dose maps in the axial plane around a linear array of multiple ^{125}I seeds were simulated [Figure 4]. The MC-simulated uncertainties of these three stent models were all within the limits recommended by the AAPM TG43U1. Since prescription doses were often defined at 0.5, 1.0, and 2.0 cm,^[6,7,17] depth dose calculations of stents of different lengths and with different activities of ^{125}I seeds were performed at 0.1, 0.5, 1.0, 1.5, and 2.0 cm from the surface of the stent [Table 2].

DISCUSSION

Over the past 10 years, several animal experiments^[18-21] and Phase I–II clinical studies^[6,7,22-24] have demonstrated the short-term efficacy and safety of intraluminal brachytherapy with ^{125}I seed-loaded stents. The favorable results of a multicenter, single-blind, randomized, Phase III trial fueled interest in the use of intraluminal brachytherapy for intraluminal malignancies.^[24] However, there are few dosimetric studies on radioactive stents, and the range of target irradiation dose reported was very broad. Thus, to allow comparisons between studies, standardization of the clinical application of ^{125}I seed-loaded radioactive stents is urgently needed.

At present, experimental TLD measurements and/or MC simulations is the standard method to accurately measure the dosimetric characteristics of radioactive brachytherapy sources. In this investigation, TG43-based brachytherapy 3D-TPS calculation was also performed for the purpose of data intercomparison.

The TPS employs a point source approximation to calculate dose distributions. When using the TPS for calculation of dose, the stent and the medium around it are simulated as water, ignoring the structure inhomogeneities with only limited dose uncertainties.^[25] The TPS in this study calculated the dose using point source simulations, which in fact agreed to be within about 2% with the full geometric simulations at all distances between 1 cm and 10 cm;^[26] thus, within this practical range, TPS agrees very well with the TLD measurements and MCNPX. Therefore, the TPS utilized by

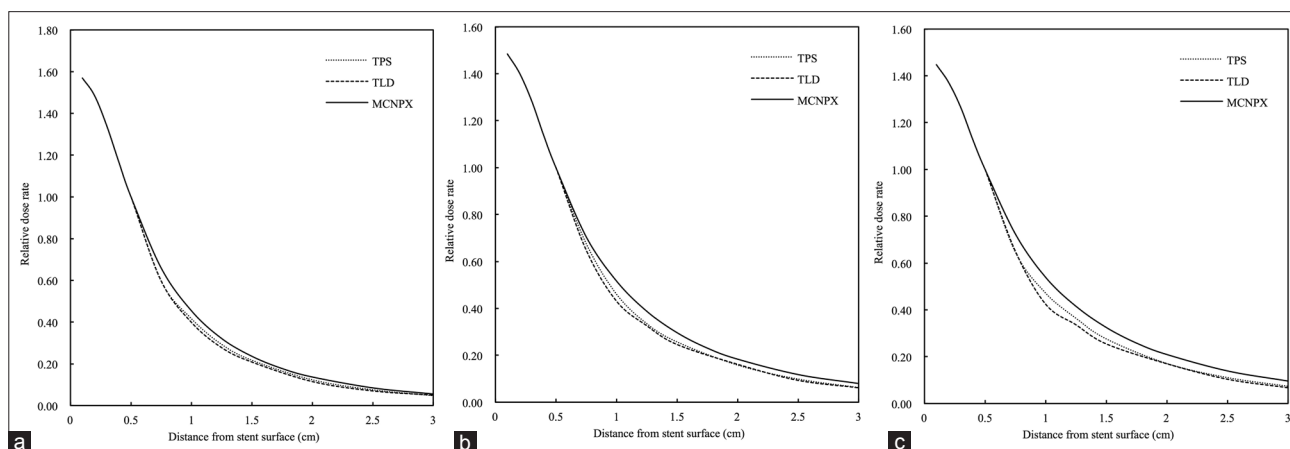


Figure 2: Comparison of radial dose rates for radioactive stent. The dose rates were normalized to the dose rate at a radial distance of 10 mm. (a-c) Stents loaded with 8, 16, and 24 ¹²⁵I seeds, respectively.

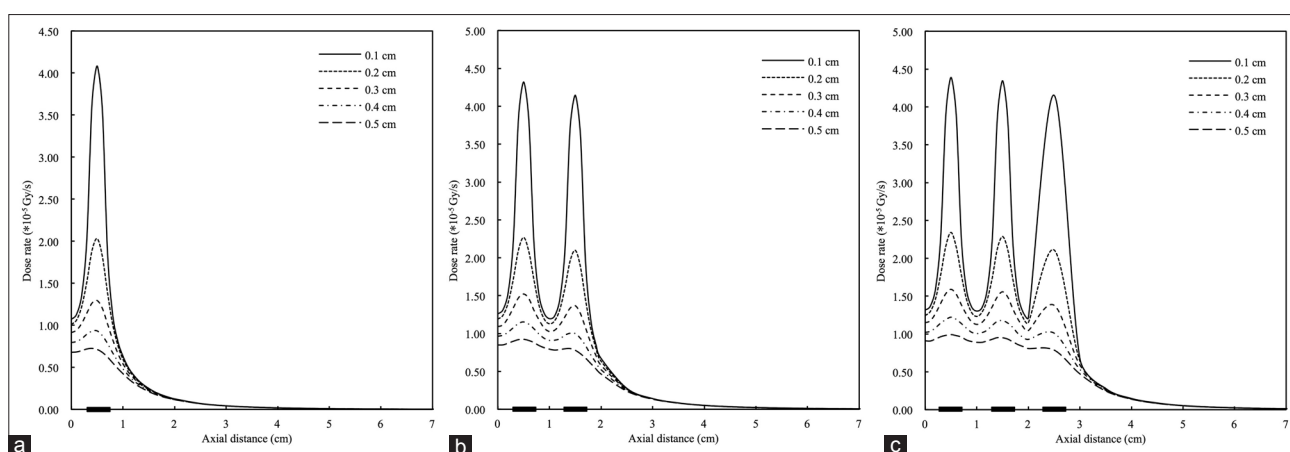


Figure 3: Monte Carlo simulated dose rates along the axial axis of the stent. The different lines represent doses at different radial distances from the surface of the stent. (a-c) Stents loaded with 8, 16, and 24 ¹²⁵I seeds, respectively.

Table 2: Cumulative radial dose distribution of different length radioactive biliary stents in different activity of ¹²⁵I seeds (Gy)

Radial distance (cm)	0.4 mCi			0.5 mCi			0.6 mCi			0.7 mCi			0.8 mCi		
	4 cm	6 cm	8 cm	4 cm	6 cm	8 cm	4 cm	6 cm	8 cm	4 cm	6 cm	8 cm	4 cm	6 cm	8 cm
0.1	79	93	97	99	117	122	119	140	146	139	163	170	158	187	195
0.5	50	63	67	63	79	84	76	94	110	88	110	118	101	126	134
1.0	23	32	36	29	41	45	34	49	57	40	57	63	46	65	72
1.5	12	19	22	15	23	27	18	28	33	21	33	38	24	37	44
2.0	7	12	14	9	14	18	10	17	20	12	20	25	14	23	28

Radial distance was from stent surface. From the formula (2), when $t \rightarrow \infty$, after seed decay completely, the total cumulative dose of the interest point is equal to $D_0(r, \theta)/\lambda$, λ is equal to $\ln 2/T_{1/2}$ ($T_{1/2} = 59.4$ days). D_0 in this table was simulated by MCNPX. MCNPX: Monte Carlo N-Particle eXtended.

us can be reliably used for clinical applications involving biliary stents.

It has been reported that, in combination therapy of esophageal cancers with stenting followed by EBRT or brachytherapy (mainly ¹⁹²Ir), dose perturbations would inevitably be caused by the esophageal stents, resulting in hot and cold spots in the esophageal mucosa.^[27,28] In our study, however, the dose measured by the TLD-GR 200A circular chips did not suggest significant deviation from

that simulated by MC, which suggested that the metal stent did not alter the brachytherapy source dose distribution in homogeneous water medium. The symmetrically arranged three radioactive sources might overcome the dose perturbations due to the metal stent. Uncertainties associated with TLD dose rate distribution measurements are due to variation between repeated measurements; relative intrinsic energy dependence; phantom material attenuation correction factor; relative absorbed DE dependence; and

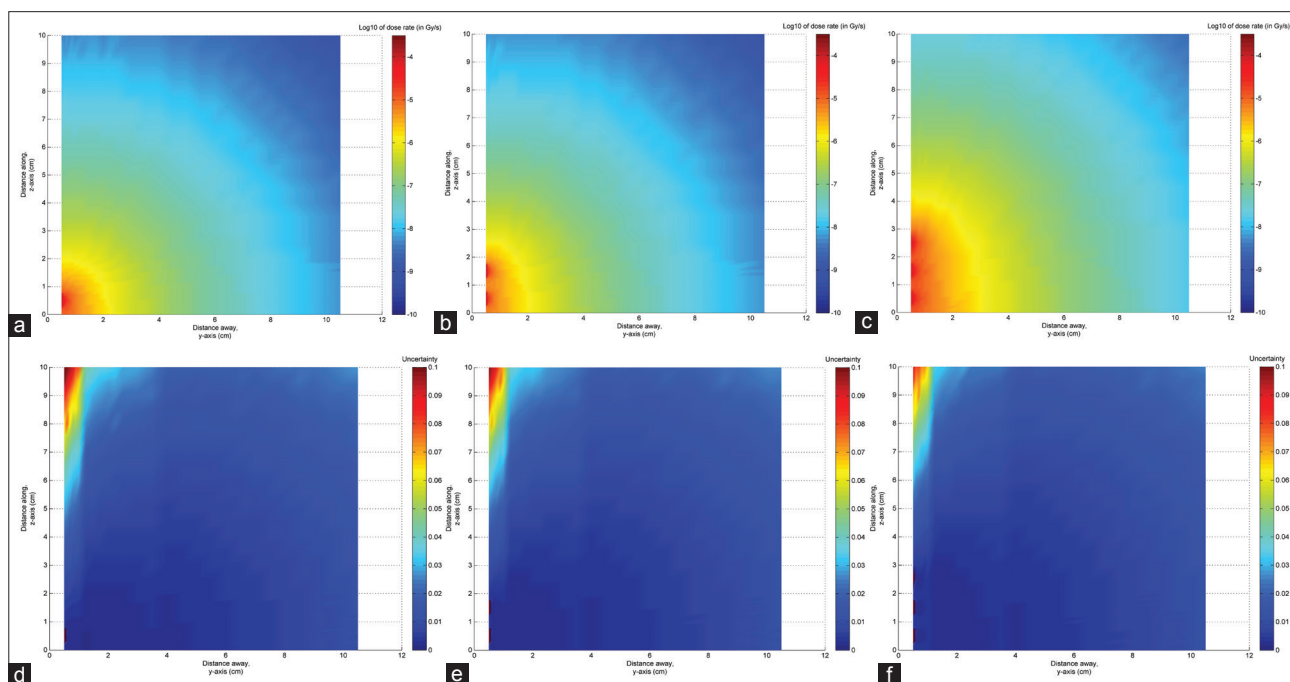


Figure 4: Dose maps were calculated for distances ranging from 0.1 cm to 10 cm radially from the stent surface and axial distances of up to 10 cm from the center of the stent. (a-c) 3D dose rate distribution for stents loaded with 8, 16, and 24 ^{125}I seeds, respectively. (d-f) The uncertainty of the measurement points of the three stent models corresponding to the Monte Carlo simulation.

TLD position relative to the sources. Due to the extremely large dose gradients and other technological limitations, doses at distances of the order of a millimeter from the radioactive stents are poorly known by TPS calculation or TLD measurement.^[8]

In our study, the 3D dose rate distributions around the radioactive stents were determined by MC simulation. To obtain the most accurate data, a full seed simulation was performed by MCNPX, though a point source simulation is a fast and efficient way to check a full seed simulation.^[26] In DE and DF input cards, we entered a point-wise response function (the American National Standards Institute standard flux-to-dose conversion factors) to modify the regular tally card. In addition, a constant was needed for use with the Fm input card to transform the result into the dose rate (Gy/s) we required. For radial dose rate distribution, the good agreement with acceptable experimental error between the calculated and measured values in water and PMMA indicated that the correct source geometry was used in the MC simulation. Based on this agreement, the simulations were performed in water in the range of 0.1–10 cm away from and along the surface of the stents. Representing the stent surface doses, cumulative radial doses at distances of 0.1 cm from stent surface were shown in Table 2, which may be used to predict the risk of bile duct wall perforation in clinical application.

In summary, our current study was purely radiophysics; TPS calculation, TLD measurement, and MC simulation were performed and were found to be in good agreement. Although the whole experiment was conducted in water-equivalent phantom, data in our evaluation may provide a theoretical basis for dosimetry for the clinical

application. More instructive data may be obtained through further *in vivo* experiments.

Acknowledgment

We would like to thank Ming Jiang for his useful comments and suggestions relating to the study design and analysis.

Financial support and sponsorship

This study was supported by a grant of the Capital Featured Clinical Application Research Project (No. Z151100004015171).

Conflicts of interest

There are no conflicts of interest.

REFERENCES

- Irving JD, Adam A, Dick R, Dondelinger RF, Lunderquist A, Roche A. Gianturco expandable metallic biliary stents: Results of a European clinical trial. *Radiology* 1989;172:321-6. doi: 10.1148/radiology.172.2.2664861.
- Válek V, Kysela P, Kala Z, Kiss I, Tomásek J, Petera J. Brachytherapy and percutaneous stenting in the treatment of cholangiocarcinoma: A prospective randomised study. *Eur J Radiol* 2007;62:175-9. doi: 10.1016/j.ejrad.2007.01.037.
- Jain S, Kataria T, Bisht SS, Gupta D, Vikraman S, Bajjal S, *et al.* Malignant obstructive jaundice – Brachytherapy as a tool for palliation. *J Contemp Brachytherapy* 2013;5:83-8. doi: 10.5114/jcb.2013.35563.
- Mattiucci GC, Autorino R, D'Agostino GR, Deodato F, Macchia G, Perri V, *et al.* Chemoradiation and brachytherapy in extrahepatic bile duct carcinoma. *Crit Rev Oncol Hematol* 2014;90:58-67. doi: 10.1016/j.critrevonc.2013.10.007.
- Mattiucci GC, Autorino R, Tringali A, Perri V, Balducci M, Deodato F, *et al.* A Phase I study of high-dose-rate intraluminal brachytherapy as palliative treatment in extrahepatic biliary tract cancer. *Brachytherapy* 2015;14:401-4. doi: 10.1016/j.brachy.2014.12.002.

6. Zhu HD, Guo JH, Zhu GY, He SC, Fang W, Deng G, *et al.* A novel biliary stent loaded with (125)I seeds in patients with malignant biliary obstruction: Preliminary results versus a conventional biliary stent. *J Hepatol* 2012;56:1104-11. doi: 10.1016/j.jhep.2011.12.018.
7. Chen Y, Wang XL, Yan ZP, Wang JH, Cheng JM, Gong GQ, *et al.* The use of ¹²⁵I seed strands for intraluminal brachytherapy of malignant obstructive jaundice. *Cancer Biother Radiopharm* 2012;27:317-23. doi: 10.1089/cbr.2011.0999.
8. Nath R, Amols H, Coffey C, Duggan D, Jani S, Li Z, *et al.* Intravascular brachytherapy physics: Report of the AAPM Radiation Therapy Committee Task Group no. 60. American Association of Physicists in Medicine. *Med Phys* 1999;26:119-52. doi: 10.1118/1.598496.
9. Chiu-Tsao ST, Schaart DR, Soares CG, Nath R; AAPM Therapy Physics Committee Task Group No 149. Dose calculation formalisms and consensus dosimetry parameters for intravascular brachytherapy dosimetry: Recommendations of the AAPM Therapy Physics Committee Task Group no. 149. *Med Phys* 2007;34:4126-57. doi: 10.1118/1.2767184.
10. Nath R, Anderson LL, Luxton G, Weaver KA, Williamson JF, Meigooni AS. Dosimetry of interstitial brachytherapy sources: Recommendations of the AAPM Radiation Therapy Committee Task Group no. 43. American Association of Physicists in Medicine. *Med Phys* 1995;22:209-34. doi: 10.1118/1.597458.
11. Rivard MJ, Coursey BM, DeWerd LA, Hanson WF, Huq MS, Ibbott GS, *et al.* Update of AAPM Task Group no. 43 Report: A revised AAPM protocol for brachytherapy dose calculations. *Med Phys* 2004;31:633-74. doi: 10.1118/1.1646040.
12. Yao LL, Lin L, Sun HT, Wang JJ, Zhou FG, Yan XQ, *et al.* Calculation of the surface radial dose distribution of radioactive biliary stent loaded with ¹²⁵I seeds by treatment planning system (in Chinese). *Natl Med J China* 2016;96:727-30. doi: 10.3760/cma.j.isn.0376-2491.2016.09.014.
13. Duggan DM, Johnson BL. Dosimetry of the I-Plant Model 3500 iodine-125 brachytherapy source. *Med Phys* 2001;28:661-70. doi: 10.1118/1.1357456.
14. Meigooni AS, Yoe-Sein MM, Al-Otoom AY, Sowards KT. Determination of the dosimetric characteristics of InterSource125 iodine brachytherapy source. *Appl Radiat Isot* 2002;56:589-99. doi: 10.1016/S0969-8043(01)00258-5.
15. Solberg TD, DeMarco JJ, Hugo G, Wallace RE. Dosimetric parameters of three new solid core I-125 brachytherapy sources. *J Appl Clin Med Phys* 2002;3:119-34. doi: 10.1120/1.1464086.
16. Rodriguez M, Rogers DW. Effect of improved TLD dosimetry on the determination of dose rate constants for (125)I and (103)Pd brachytherapy seeds. *Med Phys* 2014;41:114301. doi: 10.1118/1.4895003.
17. Yoshioka Y, Ogawa K, Oikawa H, Onishi H, Kanesaka N, Tamamoto T, *et al.* Impact of intraluminal brachytherapy on survival outcome for radiation therapy for unresectable biliary tract cancer: A propensity-score matched-pair analysis. *Int J Radiat Oncol Biol Phys* 2014;89:822-9. doi: 10.1016/j.ijrobp.2014.04.020.
18. Guo JH, Teng GJ, Zhu GY, He SC, Deng G, He J. Self-expandable stent loaded with 125I seeds: Feasibility and safety in a rabbit model. *Eur J Radiol* 2007;61:356-61. doi: 10.1016/j.ejrad.2006.10.003.
19. Liu Y, Liu JL, Cai ZZ, Lu Z, Gong YF, Wu HY, *et al.* A novel approach for treatment of unresectable extrahepatic bile duct carcinoma: Design of radioactive stents and an experimental trial in healthy pigs. *Gastrointest Endosc* 2009;69:517-24. doi: 10.1016/j.gie.2008.05.069.
20. Chen Y, Wang XL, Yan ZP, Wang JH, Cheng JM, Gong GQ, *et al.* Damage to pig bile duct caused by intraluminal brachytherapy using a (125)I ribbon. *Acta Radiol* 2013;54:272-7. doi: 10.1258/ar.2012.120214.
21. Gan Z, Jing J, Zhu G, Qin Y, Teng G, Guo J. Preventive effects of ¹²⁵I seeds on benign restenosis following esophageal stent implantation in a dog model. *Mol Med Rep* 2015;11:3382-90. doi: 10.3892/mmr.2014.3130.
22. Guo JH, Teng GJ, Zhu GY, He SC, Fang W, Deng G, *et al.* Self-expandable esophageal stent loaded with 125I seeds: Initial experience in patients with advanced esophageal cancer. *Radiology* 2008;247:574-81. doi: 10.1148/radiol.2472070999.
23. Liu Y, Lu Z, Zou DW, Jin ZD, Liu F, Li SD, *et al.* Intraluminal implantation of radioactive stents for treatment of primary carcinomas of the peripancreatic-head region: A pilot study. *Gastrointest Endosc* 2009;69:1067-73. doi: 10.1016/j.gie.2008.08.033.
24. Zhu HD, Guo JH, Mao AW, Lv WF, Ji JS, Wang WH, *et al.* Conventional stents versus stents loaded with (125) iodine seeds for the treatment of unresectable oesophageal cancer: A multicentre, randomised phase 3 trial. *Lancet Oncol* 2014;15:612-9. doi: 10.1016/S1470-2045(14)70131-7.
25. Karlsson M, Nilsson J, Lundell M, Carlsson Tedgren A. Monte Carlo dosimetry of the eye plaque design used at the St. Erik Eye Hospital for (125)I brachytherapy. *Brachytherapy* 2014;13:651-6. doi: 10.1016/j.brachy.2014.05.018.
26. Duggan DM. Improved radial dose function estimation using current version MCNP Monte-Carlo simulation: Model 6711 and ISC3500 ¹²⁵I brachytherapy sources. *Appl Radiat Isot* 2004;61:1443-50. doi: 10.1016/j.apradiso.2004.05.070.
27. Li XA, Chibani O, Greenwald B, Suntharalingam M. Radiotherapy dose perturbation of metallic esophageal stents. *Int J Radiat Oncol Biol Phys* 2002;54:1276-85.
28. Atwood TF, Hsu A, Ogara MM, Luba DG, Tamler BJ, Disario JA, *et al.* Radiotherapy dose perturbation of esophageal stents examined in an experimental model. *Int J Radiat Oncol Biol Phys* 2012;82:1659-64. doi: 10.1016/j.ijrobp.2011.02.020.